



Cite this: *Chem. Sci.*, 2020, **11**, 2982

All publication charges for this article have been paid for by the Royal Society of Chemistry

Received 21st January 2020
Accepted 7th February 2020

DOI: 10.1039/d0sc00401d

rsc.li/chemical-science

A germaaluminocene†

Lena Albers, * Patrik Tholen, Marc Schmidtman and Thomas Müller *

The reactions of dipotassium germacyclopentadienediide with two Group 13 dichlorides, Cp*BCl₂ and Cp*AlCl₂, yield two structurally different products. In the case of boron a borole complex of germanium(II) is obtained. The aluminium halide gives an unprecedented neutral germaaluminocene. Both compounds were fully characterised by multinuclear NMR spectroscopy supported by DFT computations. The molecular structure of the germaaluminocene was determined by XRD.

Introduction

The aim of utilizing readily available and environmentally benign main group element compounds for activation of unreactive materials and strong bonds instead of transition metal-based complexes became increasingly popular during the last decade.¹ We attempted to follow this lead by establishing polarised heteroalkenes **I** as they mimic the electronic situation in transition metal complexes (Fig. 1). The polarised frontier orbitals of these alkenes **I** provide the needed amphiphilic reactivity. Examples for small molecule activation by polarised heteroalkenes have already been reported.²

Our initial idea was to obtain access to polarised hetero-fulvenes **III** in which the Group 14 element is partnered with Group 13–15 elements (Scheme 1). For this reason, we studied the reaction of dipotassium germa- or silacyclopentadienediides **II**³ with a series of main group element dihalides. In several cases, we isolated rearranged products with rather unusual structures in high yields.⁴ For example, the reaction of aminoboron dichlorides with germacyclopentadienediide K₂[**1**] yielded unprecedented borole complexes of germanium(II) **2**.^{4a} The recent publication by Ruth and Sindlinger who reported the synthesis of a borole-based aluminocene **4**⁵ (Fig. 2) prompted us to communicate our own results on the reactivity of pentamethylcyclopentadiene-substituted boron and aluminium dichlorides *versus* dipotassium germacyclopentadienediide K₂[**1**] (Scheme 2).

Results and discussion

The reaction of K₂[**1**]³ with Cp*BCl₂⁶ gave the expected borole complex **2c**. The NMR spectra suggested quantitative

Institute of Chemistry, Carl von Ossietzky University Oldenburg, Carl von Ossietzky-Strasse 9-11, D-26129 Oldenburg, Federal Republic of Germany. E-mail: lena.albers@uni-oldenburg.de; thomas.mueller@uni-oldenburg.de

† Electronic supplementary information (ESI) available. CCDC 1969078. For ESI and crystallographic data in CIF or other electronic format see DOI: 10.1039/d0sc00401d

conversion and after work-up complex **2c** was isolated as a brown oil in 35% yield (Scheme 2). NMR spectroscopy evidenced the presence of the expected borole ring with a η¹-bound cyclopentadienyl substituent. Interestingly, the NMR data indicated frozen rotation around the B-Cα single bond, giving rise to ten ¹³C NMR signals for the cyclopentadienyl substituent (Table S3, ESI†). In addition, all four carbon atoms of the borole ring are magnetically non-equivalent. Even at T = 70 °C the NMR signals show no detectable line broadening. Diagnostic for the structure of the product **2c** are the high-field shifted ¹³C NMR resonances of carbon atoms C1/C4 compared to germole dianion **1**²⁻ (δ¹³C(C1/C4) = 156.2³ (**1**); 99.8, 99.3 (**2c**)). In addition, the ¹³C NMR signals of C1/C4 in borole **2c** are markedly broadened (full width at half height, ω_{1/2} = 60 Hz), due to the quadrupole moment of the neighbouring boron atom. The position of the ¹¹B NMR resonance (δ¹¹B = 37, ω_{1/2} = 283 Hz) indicates tri-coordination for the boron atom. The boron

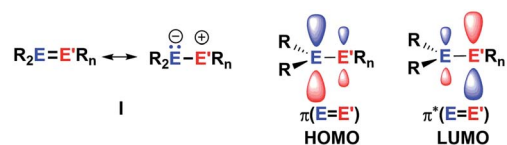
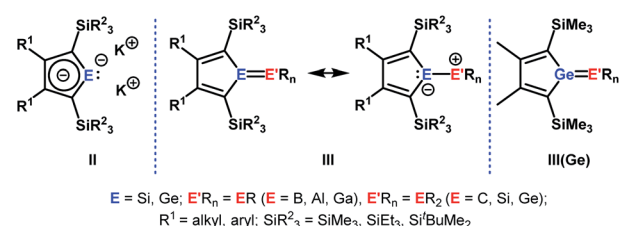


Fig. 1 Polarised heteroalkenes **I** and a sketch of their frontier orbitals.



Scheme 1 Dipotassium sila- or germacyclopentadienediides **II**, polarised heteroalkenes **III** and **III(Ge)**.





Fig. 2 Main group compounds relevant for the discussion.



Scheme 2 Synthesis of borole germanium complex **2c** and germaaluminocene **3** from dipotassium germacyclopentadienediide $K_2[1]$ by salt metathesis.

resonance is significantly deshielded compared to that of borocenium tetrachloroaluminate $5[AlCl_4]$ ($\delta^{11}B = -42$)⁷ which discards the possibility of η^5 -coordination. These NMR chemical shifts are all close to those reported previously for amino-substituted borole complexes **2a** and **2b**^{4a} (Table S3[†]). In addition, NMR chemical shift calculations using a DFT-optimised molecular structure of complex **2c** provide ¹³C and ¹¹B chemical shifts that are close to the experiment (*i.e.* $\delta^{11}B^{calc} = 30$) and strongly support our structural proposal for **2c** (Table S3[†]).

Applying the same conditions to the reaction of $K_2[1]$ with Cp^*AlCl_2 ,⁸ we noticed complete conversion of both reactants to a single product according to NMR spectroscopy. Due to its high solubility, we isolated compound **3** by crystallization in only

moderate yields of 28% as yellow solid. The NMR data indicated a molecular structure very different from that of the germanium borole complex **2c**. Compound **3** is characterised by a relative sharp, high-field shifted ²⁷Al NMR signal at $\delta^{27}Al = -77$ ($\omega_{1/2} = 703$ Hz). The number of signals in the ¹H and ¹³C NMR spectra suggests a highly symmetric structure for compound **3** and the two ¹³C NMR resonances of the Cp* ligand are in the typical range of η^5 -coordination ($\delta^{13}C = 114.9, 10.8$) (Table S3[†]). Even at temperatures as low as $T = -90$ °C, all Cp*-carbon atoms are magnetically equivalent, which supports the presence of a η^5 -bound Cp*-substituent (see ESI[†]). The ¹³C NMR chemical shifts of the heterole ring are decisively different from that of the borole ring in **2c**. In particular, the carbon atoms C1/C4 are significantly deshielded compared to the borole complex **2c** or compared to the germole dianion **1**²⁻ ($\delta^{13}C(C1/4) = 167.0$ (**3**); 99.8, 99.3 (**2c**) and 156.2 (**1**²⁻)). These ¹³C and in particular ²⁷Al NMR data are also different from those reported for the dilithium aluminacyclopentadienediide $Li_2[6]$, ($\delta^{27}Al = 198$ ($\omega_{1/2} = 7000$ Hz), Table S3[†])⁹ or for the tris- η^1 -cyclopentadienyl-substituted alane **7** ($\delta^{27}Al = 64$).¹⁰ They are however close to that of η^5 -coordinated cyclopentadienyl aluminium compounds **8**⁺-**11** ($\delta^{27}Al = -59$ to -150)¹¹ which suggests a η^5 -coordination of the cyclopentadienyl substituent to the aluminium atom for complex **3**. The NMR data is consistent with a sandwich structure of compound **3** as depicted in Scheme 2. Further support comes from NMR chemical shift calculations for a DFT-optimised sandwich structure **3** which predict aluminium and carbon NMR chemical shifts that are very close to the experimental values ($\delta^{27}Al^{calc} = -71$, Table S3[†]).

Yellow crystals of **3**, suitable for X-ray diffraction (XRD) analysis were obtained from hexanes. In the solid state compound **3** adopts a sandwich structure with a η^5 -coordinated Cp* ligand and with close contacts to all five atoms of the germole ring (Fig. 3). All germole-C-Al distances (213–228 pm) and the Ge/Al separation (248.8 pm) are significantly shorter than the respective sum of the van der Waals radii $\Sigma vdw(C/Al) = 354$ pm; $\Sigma vdw(Ge/Al) = 395$ pm).¹² The Ge–Al distance matches even that of Ge–Al single bonds in germyl-alanes¹³ and -alanates¹⁴ (244.9–254.5 pm, theoretically predicted: 247 pm¹⁵). The distance

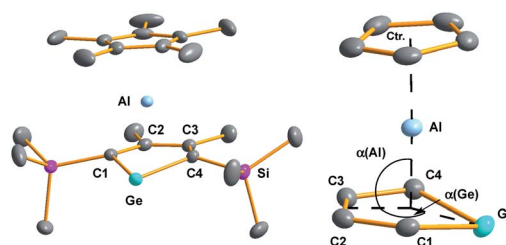


Fig. 3 Left: Molecular structure of **3** in the crystal (Hydrogen atoms are omitted; thermal ellipsoids at 50% probability). Right: Coordination environment of the aluminium atom. Selected atom distances [pm] and angles [°]: Ge–C1 199.91(10), Ge–C4 200.02(10), Al–C1 212.87(10), Al–C2 227.18(10), Al–C3 227.58(10), Al–C4 214.16(11), Ge–Al 248.78(4), C1–C2 144.70(13), C2–C3 142.12(14), C3–C4 144.56(13), Al–Ctr. 186.64(3), Al–C(Cp*) 217–228, $\alpha(Ge)$ 165.638(9); $\alpha(Al)$ 91.628(10).





Fig. 4 Selected germole dianion metal complexes.

between the centre of the Cp* ring and the aluminium atom (186.6 pm) is only slightly larger than that found for the Cp*Al(i) complex **9**^{11c} but significantly smaller than found for monomeric Cp*Al(i) **11**¹⁶ (see Table S2[†]).

The planes defined by the Cp* ring and by the four carbon atoms of the germole ligand are aligned almost parallel (interplanar angle 3.3°). The C–C bond lengths in the germacycle indicate delocalization (142.1–144.7 pm). Compared to the germole dianion **1**²⁻ in the triple ion pair K₂[**1**] (139.5–142.0 pm),³ or in the germole dianion hafnium complexes **12** (134.7–142.8 pm)¹⁷ or **13** (140.7–144.5 pm) (Fig. 4),^{4b} all bonds in the germole ring of **3** are slightly elongated, indicating electron transfer from the germole ring to the aluminium atom (Fig. 3).

Quantum mechanical calculations at the M06-2X/6-311+G(d,p) level of theory were performed to investigate the bonding situation in neutral germaaluminocenes **3** and **3M** (**3M** is a close model to **3**, in which all substituents at the germole ring and at the cyclopentadiene ring have been replaced by hydrogen atoms).¹⁸ The analysis of the frontier molecular orbitals suggests a substantial germylene character of the sandwich complex **3M**. This is shown by surface diagrams of the frontier orbitals which indicate a significant contribution of an in-plane lone pair at germanium to HOMO–1 (Fig. 5). In addition, the 4p(Ge) atomic orbital dominates the LUMO and



Fig. 5 Calculated surface diagrams of frontier molecular orbitals of germaaluminocene **3M** (M06-2X/6-311+G(d,p), isodensity value 0.04).



Fig. 6 Calculated WBIs of pertinent bonds and NBO group charges q of complexes **3**, K₂[**1**], **8**⁺ and aluminium methyl compounds (M06-2X/6-311+G(d,p)).

the LUMO+1. The HOMO is essentially a combination of an π -orbital of the germole cycle that is polarised towards the germanium atom and atomic orbitals of the aluminium. The results of a natural bond orbital (NBO) analysis for complex **3** indicate significant charge transfer from the germole ring to the aluminium atom as shown by the calculated NBO group charges (Fig. 6). The covalent character of the aluminium/germole interaction is supported by the calculated Wiberg bond indices (WBI).¹⁹ These exceed those calculated for the ionic interaction between the potassium ions and the germole ring for K₂[**1**] (Fig. 6). In particular, the WBIs for the C1/C4–Al linkages are larger than those of C(Cp*)–Al bonds in **8**⁺ and close to those predicted for the Al–C bond in Me–Al(i) (Fig. 6).

This covalent bonding is visualised by a natural localised molecular orbital (NLMO, Fig. 7a), which indicates the electron delocalisation between atomic orbitals of the aluminium and π -type orbitals of the germole ligand. The complementary analysis of the calculated electron density of germaaluminocene **3M** in the framework of the quantum theory of atoms in molecules (QTAIM) finally reveals a consistent picture with bond paths between the aluminium atom and the carbon atoms C1/4 and a valence shell charge concentration (VSCC) between the aluminium atom and the germanium atom (Fig. 7b).



Fig. 7 (a) Surface diagram of the NLMO of **3M** showing the interaction between the germole ring and the CpAl fragment (surface value 0.04, hydrogen atoms omitted). (b) Molecular graph of **3M** projected on a contour plot of the Laplacian of the electron density in the molecular mirror plane (M06-2X/6-311+G(d,p)).





Scheme 3 Resonance representations of neutral germaaluminocene 3M.

On the basis of our theoretical results we suggest a delocalised bonding scheme for model germaaluminocene compound **3M** and likewise for the experimentally investigated compound **3**. Scheme 3 shows the three extreme Lewis forms of the delocalisation of the bonding situation in the germaaluminocene.

In the course of our computational investigation of possible reaction channels for the formation of germanium borole or alumole complexes (**2c** and **14**) or germaborocene or -aluminocene sandwich compounds (**15** and **3**), we found that structures with an Y-shaped arrangement²⁰ around the two heteroatoms, as it is shown by boraalkene **16**²¹ or borasilene **17**,²² are only high lying transition states (see ESI† for a more extensive description of the corresponding potential energy surfaces). This is surprising, in view of the recent isolation of an almost linear boragermene **18**^{2c} by Rao and Kinjo, who used an amino substituent at the boron atom (Fig. 9).

As reported previously we synthesised borole complexes of germanium(II) **2a** and **2b** from the reaction of a germacyclopentadienediide **1**²⁻ with amino boron dichlorides.^{4a} Now, we found the same structural motif when using the Cp* substituent at the boron atom. This suggests that the germacyclopentadienyl fragment, used in the chemistry presented here, has a significant effect on the reaction outcome.

In agreement with the exclusive formation of the borole germanium(II) complex **2c**, we found that **2c** is significant more stable than the isomeric germaborocene **15** ($\Delta E = 63 \text{ kJ mol}^{-1}$,

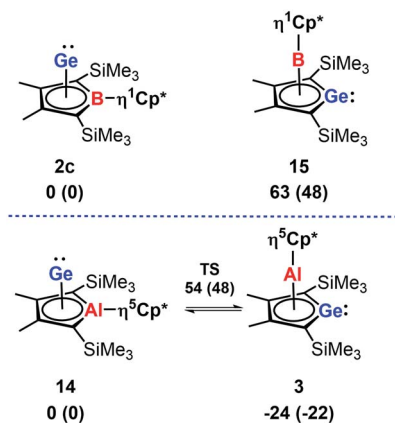


Fig. 8 Relative energies ΔE and relative free Gibbs enthalpies at $T = 298 \text{ K}$ ΔG^{298} (in brackets) of isomeric borole **2c** and alumole **14** complexes and germole complexes **15** and **3**.

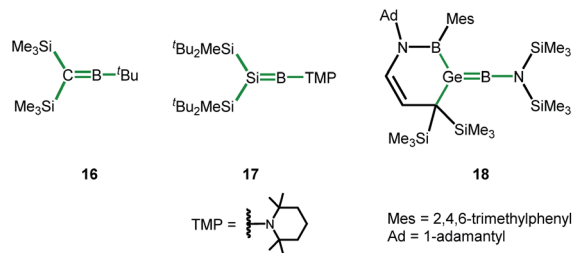


Fig. 9 Y-shaped Group 14 boraalkenes relevant for the discussion (Y-shape arrangement indicated by green bonds).

Fig. 8). The situation is different for the isomeric aluminium compounds **3** and **14**. In qualitative agreement with the isolation of the germaaluminocene **3** (Fig. 8), it is more stable than the alumole germanium(II) complex **14** by $\Delta E = 24 \text{ kJ mol}^{-1}$. We notice however that their energy difference is significantly smaller. Moreover, the barrier for the interconversion **3** \rightarrow **14** (78 kJ mol^{-1}) is relatively small (Fig. 8). These computational results for the aluminium compounds indicate the possibility to influence the product formation significantly by substituent effects. Decisive for the higher stability of the germametalloocene **3** vs. the metallole Ge(II) complex **14** is the larger size of the aluminium atom compared to the boron atom in the isomer pair **2c/15**. Its inclusion into the delocalised metallole cycle is disfavoured due to the misfit of $3p(\text{Al})$ and $2p(\text{C})$ orbitals but its larger size facilitates the η^5 -coordination to the Cp* ligand.^{7,9,23}

Conclusions

In agreement with previous results, the reaction of $\text{K}_2[1]$ Cp*BCl₂ gives a borole complex of Ge(II) **2c**. The respective reaction of $\text{K}_2[1]$ with Cp*AlCl₂ provides access to the neutral germaaluminocene **3**, which represents a new class of aluminium π -complexes. Similar to aluminocenium cation **8**^{11a,24} and boraaluminocene **4**,⁵ germaaluminocene **3** shows a η^5, η^5 -coordination of both five-membered rings. In contrast to these previous examples, germaaluminocene **3** exhibits a free electron pair and a low-lying acceptor orbital at the germanium atom, which suggests additional germylene-like reactivity.

The small energy difference between the germole **3** and isomeric alumole **14** structures and the small energetic barriers for their interconversion imply that also the synthesis of alumole complexes of Ge(II) is in reach, when substituent effects are employed advantageously.

Conflicts of interest

There are no conflicts to declare.

Acknowledgements

This work was supported by the Deutsche Forschungsgemeinschaft (DFG-Mu1440/13-1, INST 184/108-1 FUGG).



Notes and references

- 1 (a) P. P. Power, *Nature*, 2010, **463**, 171–177; (b) G. D. Frey, V. Lavallo, B. Donnadieu, W. W. Schoeller and G. Bertrand, *Science*, 2007, **316**, 439.
- 2 (a) T. Kosai and T. Iwamoto, *Chem.–Eur. J.*, 2018, **24**, 7774–7780; (b) F. Dahcheh, D. Martin, D. W. Stephan and G. Bertrand, *Angew. Chem., Int. Ed.*, 2014, **53**, 13159–13163; (c) B. Rao and R. Kinjo, *Angew. Chem., Int. Ed.*, 2019, **59**, 3147–3150.
- 3 Z. Dong, C. R. W. Reinhold, M. Schmidtman and T. Müller, *Organometallics*, 2018, **37**, 4736–4743.
- 4 (a) P. Tholen, Z. Dong, M. Schmidtman, L. Albers and T. Müller, *Angew. Chem., Int. Ed.*, 2018, **57**, 13319–13324; (b) Z. Dong, K. Bedbur, M. Schmidtman and T. Müller, *J. Am. Chem. Soc.*, 2018, **140**, 3052–3060; (c) Z. Dong, C. R. W. Reinhold, M. Schmidtman and T. Müller, *J. Am. Chem. Soc.*, 2017, **139**, 7117–7123; (d) Z. Dong, C. R. W. Reinhold, M. Schmidtman and T. Müller, *Angew. Chem., Int. Ed.*, 2016, **55**, 15899–15904.
- 5 C. P. Sindlinger and P. N. Ruth, *Angew. Chem., Int. Ed.*, 2019, **58**, 15051–15056.
- 6 P. Jutzi, B. Krato, M. Hursthouse and A. Howes, *Chem. Ber.*, 1987, **120**, 565.
- 7 A. Voigt, S. Filipponi, C. L. B. Macdonald, J. D. Gorden and A. H. Cowley, *Chem. Commun.*, 2000, 911–912.
- 8 H.-J. Koch, S. Schulz, H. W. Roesky, M. Noltemeyer, H.-G. Schmidt, A. Heine, R. Herbst-Irmer, D. Stalke and G. M. Sheldrick, *Chem. Ber.*, 1992, **125**, 1107–1109.
- 9 T. Agou, T. Wasano, P. Jin, S. Nagase and N. Tokitoh, *Angew. Chem., Int. Ed.*, 2013, **52**, 10031–10034.
- 10 J. D. Fisher, P. H. M. Budzelaar, P. J. Shapiro, R. J. Staples, G. P. A. Yap and A. L. Rheingold, *Organometallics*, 1997, **16**, 871–879.
- 11 (a) R. W. Schurko, I. Hung, C. L. B. Macdonald and A. H. Cowley, *J. Am. Chem. Soc.*, 2002, **124**, 13204–13214; (b) J. D. Gorden, C. L. B. Macdonald and A. H. Cowley, *Chem. Commun.*, 2001, 75–76; (c) J. D. Gorden, A. Voigt, C. L. B. Macdonald, J. S. Silverman and A. H. Cowley, *J. Am. Chem. Soc.*, 2000, **122**, 950–951; (d) C. Dohmeier, H. Schnöckel, U. Schneider, R. Ahlrichs and C. Robl, *Angew. Chem., Int. Ed.*, 1993, **32**, 1655–1657; (e) J. Gauss, U. Schneider, R. Ahlrichs, C. Dohmeier and H. Schnöckel, *J. Am. Chem. Soc.*, 1993, **115**, 2402–2408.
- 12 M. Mantina, A. C. Chamberlin, R. Valero, C. J. Cramer and D. G. Truhlar, *J. Phys. Chem. A*, 2009, **113**, 5806–5812.
- 13 J. D. Erickson, J. C. Fettingler and P. P. Power, *Inorg. Chem.*, 2015, **54**, 1940–1948.
- 14 (a) T. Habereeder, H. Nöth and M. Suter, *Z. Naturforsch., B: Chem. Sci.*, 2009, **64**, 1387; (b) T. Habereeder, K. Knabel and H. Nöth, *Eur. J. Inorg. Chem.*, 2001, **2001**, 1127–1129.
- 15 P. Pykkö and M. Atsumi, *Chem.–Eur. J.*, 2009, **15**, 12770–12779.
- 16 A. Haaland, K.-G. Martinsen, S. A. Shlykov, H. V. Volden, C. Dohmeier and H. Schnöckel, *Organometallics*, 1995, **14**, 3116–3119.
- 17 J. M. Dysard and T. D. Tilley, *J. Am. Chem. Soc.*, 2000, **122**, 3097–3105.
- 18 (a) *The Programme Gaussian 16 Revision A.03* Gaussian Inc., Wallingford CT, 2016 was used; (b) For details see the ESI.†
- 19 K. B. Wiberg, *Tetrahedron*, 1968, **24**, 1083–1096.
- 20 The term “Y-shaped arrangement” indicates the spatial arrangement of the three substituents around the double bond, for example, of vinyl cations or boragermenes.
- 21 R. Boese, P. Paetzold, A. Tapper and R. Ziembinski, *Chem. Ber.*, 1989, **122**, 1057–1060.
- 22 N. Nakata and A. Sekiguchi, *J. Am. Chem. Soc.*, 2006, **128**, 422–423.
- 23 (a) O. Kwon and M. L. McKee, *J. Phys. Chem. A*, 2001, **105**, 10133–10138; (b) J. O. C. Jimenez-Halla, E. Matito, M. Solà, H. Braunschweig, C. Hörl, I. Krummenacher and J. Wahler, *Dalton Trans.*, 2015, **44**, 6740–6747.
- 24 C. L. B. Macdonald, J. D. Gorden, A. Voigt, S. Filipponi and A. H. Cowley, *Dalton Trans.*, 2008, 1161–1176.

